HGT

Long-Term Survival and Myocardial Function Following Systemic Delivery of Delandistrogene Moxeparvovec in DMD^{MDX} Rats

Stephen Baine,† Chris Wier,† Luke Lemmerman, Grace Cooper-Olson, Amber Kempton, Alex Haile, Julian Endres, Alessandra Fedoce, Ellyn Nesbit, Louise R. Rodino-Klapac, and Rachael A. Potter*

Sarepta Therapeutics, Inc., Cambridge, Massachusetts, USA.
†Co-first authors.
This research was completed at the Genetic Therapies Center of Excellence in Columbus, Ohio, USA. This research used DMD^{MDX} rats, which were generated and characterized in the following publication: Larcher T, et al. Characterization of dystrophin-deficient rats: a new model for Duchenne muscular dystrophy. PLoS One. 2014; 9:e110371.

Delandistrogene moxeparvovec is a gene transfer therapy for Duchenne muscular dystrophy (DMD) that uses an adeno-associated viral vector to deliver a micro-dystrophin transgene to skeletal and cardiac muscle. This study evaluated the long-term survival and cardiac efficacy of delandistrogene moxeparvovec in a DMD-mutated (DMD^{MDX}) rat model of DMD-related cardiomyopathy. DMD^{MDX} male rats, aged 21–42 days, were injected with 1.33×10^{14} viral genomes/kilogram (vg/kg) delandistrogene moxeparvovec and followed for 12, 24, and 52 weeks. Ambulation was recorded *via* the Photobeam Activity System, whereas echocardiograms, cardiomyocyte contractility, calcium handling, and histological analysis of fibrosis were used to evaluate cardiac disease at 12-, 24-, and 52-weeks post-treatment. A separate cohort of rats was used to assess the impact of delandistrogene moxeparvovec on survival. Treatment with delandistrogene moxeparvovec extended median survival in DMD^{MDX} rats to >25 months versus the 13-month median survival in saline-control-treated DMD^{MDX} rats. Compared with saline control, delandistrogene moxeparvovec therapy elicited statistically significant improvements across cardiac parameters approaching wild-type values with additional benefits in mobility, histopathology, and fibrosis observed. Transgene expression was maintained up to >25 months and micro-dystrophin expression was broadly distributed across skeletal and cardiac muscle. Taken together, these findings demonstrate long-term cardiac efficacy and improved survival following delandistrogene moxeparvovec treatment in DMD^{MDX} rats.

Keywords: Vectors—AAV, disease models—muscle/connective tissue/bone, cell-based therapies, clinical development—IND-enabling studies

INTRODUCTION

Duchenne muscular dystrophy (DMD) is a rare, X-linked neuromuscular disease caused by mutations in the dystrophin (*DMD)* gene that disrupt the production of functional dystrophin protein.[1] The absence or insufficient production of dystrophin can lead to myofiber damage, muscle degeneration, and necrosis, which results in progressive muscle weakness and wasting.[2,3] DMD is associated with early mortality often from cardiac or respiratory failure, with a life expectancy of approximately 30 years.[4,5] Cardiomyopathy has become the most common cause of death in patients with DMD.[6,7] Dystrophin plays various roles in the cardiac myocyte, but the underlying DMD pathophysiology is in part linked to calcium dysregulation.[8] Calcium excess due

Correspondence: Dr. Rachael A. Potter, Sarepta Therapeutics, Inc., 215 First Street, Cambridge, MA 02142, USA. E-mail: RPotter@Sarepta.com

DOI: 10.1089/hum.2024.013

to membrane instability is a primary mechanistic contributor to disease progression.[8]

Delandistrogene moxeparvovec is an adeno-associated viral (AAV) vector-based gene therapy approved in the United States for the treatment of patients with DMD at least 4 years of age with a confirmed mutation in the *DMD* gene, regardless of ambulatory status.[9] As of May 2024, delandistrogene moxeparvovec is approved in the UAE, Qatar, Kuwait, Bahrain, and Oman for the treatment of ambulatory pediatric patients with DMD aged 4–5 years with a confirmed mutation in the *DMD* gene.[9–14] Delandistrogene moxeparvovec has been designed to address DMD using a recombinant AAV serotype rh74 (rAAVrh74) vector for targeted production of delandistrogene moxeparvovec micro-dystrophin, an engineered dystrophin protein that retains key functional domains of the wild-type (WT) protein (Supplementary Fig. S1).[15]

As clinical trial data primarily focus on the functional evaluation of ambulation in patients, there is a need to better understand cardiac outcomes following treatment with delandistrogene moxeparvovec. In pre-clinical studies using *mdx* mice, reductions in fibrosis and improvements in skeletal muscle function were observed following systemic delivery of delandistrogene moxeparvovec.[16,17] Although the *mdx* mouse is a valuable genetic and biochemical model, it manifests a mild cardiac phenotype relative to human disease.[17–21] DMD^{MDX} rats are a valuable alternative model as they demonstrate cardiac dysfunction that more closely resembles the cardiac phenotype seen in patients with DMD.[17,18]

Here we report the long-term therapeutic benefit of delandistrogene moxeparvovec in DMD^{MDX} rats, including improved functional and cardiac outcomes with prolonged survival.

MATERIALS AND METHODS

Ethics

All procedures were in compliance with the Animal Welfare Act, the Guide for the Care and Use of Laboratory Animals, and were approved by the local institution's animal care and use committee.

Animal model

Male Sprague-Dawley DMD^{MDX} and WT rats, obtained from the University of Nantes (France)[17] and Taconic Biosciences, were intravenously administered saline or delandistrogene moxeparvovec at 21–42 days of age and euthanized (Euthasol 150–200 mg/kg; Supplementary Table S1) for tissue collection at predetermined time points. Operators of all functional outcomes were blinded to the treatment group (see Supplementary Table S2 for an overview of the study design and outcomes; see supplementary methods for further details).

Delandistrogene moxeparvovec expression, histology, and biochemical analyses

Details on the following methods can be found in Supplementary Appendix SA1: biodistribution analysis using droplet digital polymerase chain reaction, western blot analysis, histology and morphological analysis, immunofluorescence, and serum analysis.

Activity cage assessments

Activity cage assessments were performed at 10 and 50 weeks. Ambulation was measured by light beam breaks over a set period using the Photobeam Activity System-Open Field Activity Cage (San Diego Instruments). Animals were placed in the open field for monitoring of unprovoked movement.

Echocardiography

For information on how rats were anesthetized, see Supplementary Appendix SA1. For echocardiography, parasternal long and short axis views were obtained. Apical four-chamber views were obtained in a subset of animals. M-mode and apical four-chamber images were analyzed using Vevo LAB Systems software. Echocardiography personnel were blinded to the treatment group.

Cardiomyocyte isolation

Individual cardiomyocytes were isolated as previously described.[22] Briefly, rodent hearts were excised and cannulated through the aorta for perfusion with ice-cold calcium-free Tyrode's solution. Cannulated hearts were transferred to a perfusion-flow Langendorff apparatus containing calcium-free Tyrode's solution set to maintain a temperature of approximately 37°C. Hearts were perfused for 5–15 min before the solution was changed to Tyrode's solution containing Liberase TH (Roche). Following enzymatic digestion, hearts were removed and minced in a dish containing the perfusion solution. The resultant cell solution was filtered and mixed with Tyrode's solution containing bovine serum albumin to neutralize enzymatic activity.

Cardiomyocyte functional analysis

Freshly isolated cardiomyocytes were incubated with Fura-2 AM dye for 20–30 min. Following loading, myocytes were allowed 15–20 min for de-esterification. The cell solution was placed in a laminin-coated microwell dish, and intracellular calcium transient and sarcomere shortening measurements were obtained by electrical field stimulation of 0.5–2 Hz (Supplementary Table S3) with the IonOptix High Throughput System (HTS). For Fura dye measurements, data were captured using the IonOptix HTS with a microscope supplemented with a dual-excitation LED light source and photomultiplier detector for simultaneous ratio metric calcium measurements, as previously described.[23]

Operators performing cardiomyocyte functional analysis were blinded to the treatment group.

Statistical analysis

Normality was determined by the Shapiro–Wilks test. If necessary to meet parametric assumptions, data were transformed using a log10 transformation. If the data set was unable to be transformed to fit a normal distribution, the raw data set was used for analysis. For parametric data sets, data were analyzed using a one- or two-way analysis of variance to determine the main effect of the independent variable(s) (*e.g.,* group, time point). If a significant effect was observed for the independent variable(s), a *post hoc* Tukey test was performed to compare differences between groups. For non-parametric data sets, data were analyzed using a Kruskal–Wallis test to determine the main effect of the independent variable(s). If a significant effect was observed for the independent variable(s), a *post hoc* Dunn's test was performed to compare differences between groups. Data comparisons were considered significantly different when $p < 0.05$.

RESULTS

Overview of study design and study outcomes

Supplementary Tables S1 and S2 provide a summary of dosing cohorts and an overview of the study design including the study outcomes measured. Briefly, Male Sprague-Dawley DMD^{MDX} and WT rats from 21 to 42 days of age were intravenously administered saline or delandistrogene moxeparvovec and subsequently euthanized at predetermined time points for tissue collection (Supplementary Table S2). Activity cage assessments were performed to measure ambulation. Echocardiography was conducted to assess cardiac function, and isolated cardiomyocytes were used for functional analysis, including calcium transient and sarcomere shortening measurements (Supplementary Tables S3 and S4). A separate cohort of rats was used to assess the impact of delandistrogene moxeparvovec on survival (Fig. 1A).

Survival

The overall benefit of delandistrogene moxeparvovec treatment was examined over 2.5 years in DMD^{MDX} rats. Without intervention, survival in DMD^{MDX} rats was <17 months, with a median survival of 13 months (Fig. 1A). Treatment with delandistrogene moxeparvovec (1.33×10^{14} viral genomes/kilogram [vg/kg]) extended median survival in DMD^{MDX} rats to >25 months. To examine the long-term treatment effects of delandistrogene moxeparvovec in the survival cohort of DMD^{MDX} rats, vector biodistribution (Supplementary Fig. S2A) and western blot analysis (Fig. 1B) were performed in selected skeletal muscles (triceps, gastrocnemius, and tibialis anterior) and cardiac tissues. In the selected samples, delandistrogene moxeparvovec was detected at varying levels, with the highest levels found in the heart (Supplementary Fig. S2A). Western blot analysis showed robust delandistrogene moxeparvovec micro-dystrophin expression in the selected skeletal muscles and heart tissue examined (Fig. 1B). Of note, representative western blot images showed no dystrophin protein expression in livers from rats treated with delandistrogene moxeparvovec (Supplementary Fig. S2B). These data demonstrate that in DMD^{MDX} rats, treatment with delandistrogene moxeparvovec provided sustained expression of the micro-dystrophin protein and extended survival to >25 months.

Delandistrogene moxeparvovec transgene and micro-dystrophin expression

Delandistrogene moxeparvovec biodistribution. The second arm of the study was limited to 1 year to evaluate the cardiac efficacy of delandistrogene moxeparvovec. Vector biodistribution analysis was performed at 12, 24, and 52 weeks, indicative of short-, intermediate-, and long-term delandistrogene moxeparvovec treatment, respectively. Delandistrogene moxeparvovec vector DNA was detected at varying levels in all collected tissue, with the highest levels in the liver, followed by the heart, and was observed broadly throughout skeletal muscle (triceps, gastrocnemius, and tibialis anterior) (Fig. 2A). Importantly, vector transduction was maintained over 52 weeks, with no significant differences in copies per nucleus between 12, 24, and 52 weeks. These results support the targeted expression and durability of delandistrogene moxeparvovec treatment with the use of a cardiac/muscle-specific promoter over 52 weeks.

Delandistrogene moxeparvovec micro-dystrophin expression. Delandistrogene moxeparvovec micro-dystrophin levels were examined by western blot and quantified as percentage of normal control (Fig. 2B and C). Treatment led to muscle and cardiac micro-dystrophin expression at 12-, 24-, and 52-weeks post dosing (Fig. 2B, C, and D), with the highest level of expression achieved in cardiac tissue (Fig. 2B, C, and D). No significant changes in expression levels were observed over time in any tissue, suggesting sustained protein expression up to 52 weeks following treatment with delandistrogene moxeparvovec (Fig. 2B and C).

Delandistrogene moxeparvovec micro-dystrophin expression and localization in treated DMD^{MDX} rats was examined by immunofluorescence at 12-, 24-, and 52-weeks post-treatment. Treatment led to substantial micro-dystrophin expression in skeletal muscles (tibialis anterior, triceps, and gastrocnemius) (Fig. 2D and E). A qualitative examination of cardiac tissue revealed membrane localized micro-dystrophin restoration following treatment at all

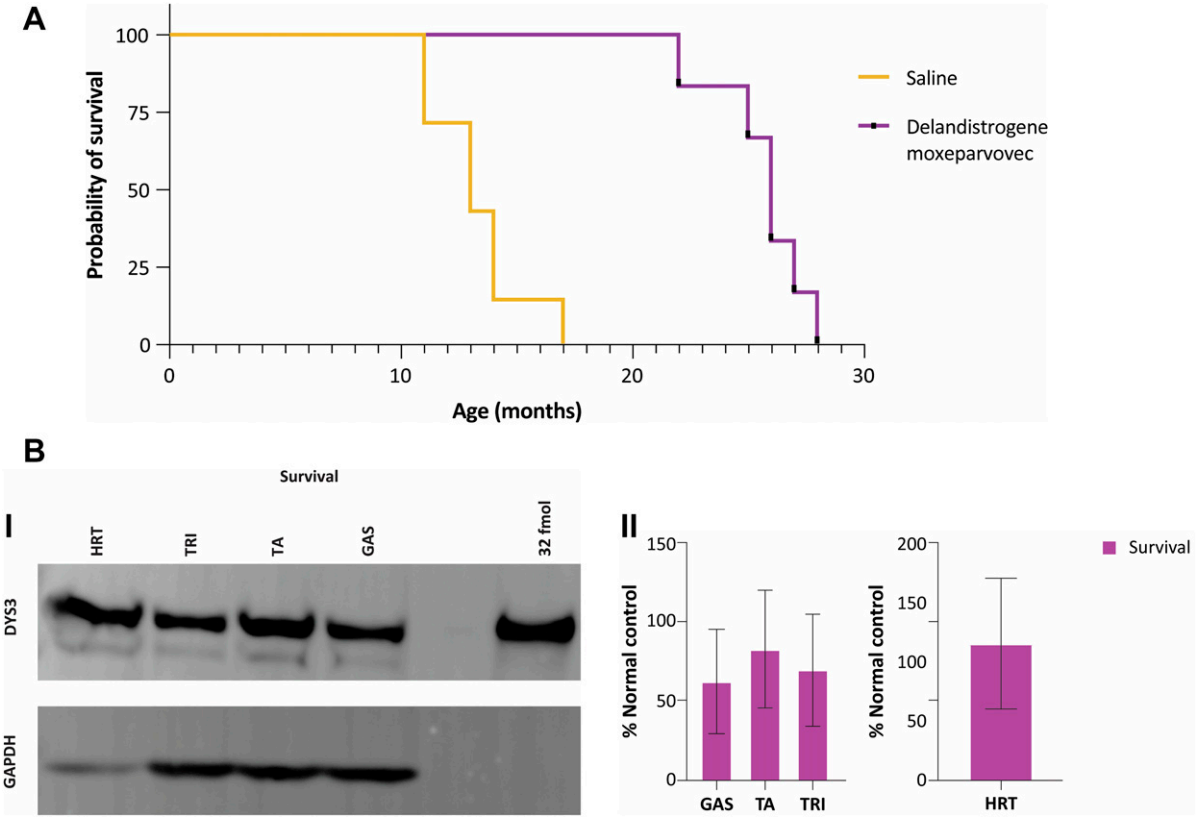

Figure 1. Survival and long-term durability analysis in DMD^{MDX} rats following treatment with delandistrogene moxeparvovec. **(A)** Representative survival curve for DMD^{MDX} rats treated with delandistrogene moxeparvovec and saline. **(B, I)** Representative western blot images in delandistrogene moxeparvovec-treated skeletal and cardiac muscle; corresponding protein bands illustrate expression of delandistrogene moxeparvovec micro-dystrophin. **(B, II)** Western blot quantification of delandistrogene moxeparvovec micro-dystrophin protein expression in muscle and heart represented as percentage (%) of normal control at the endpoint. Bars represent mean ± SD. No statistical analysis was performed for this data set. Survival saline-treated cohort, $n = 7$; survival delandistrogene moxeparvovec-treated cohort, $n = 6$. DMD, Duchenne muscular dystrophy; DYS3, dystrophin antibody 3; fmol, femtomole; GAPDH, glyceraldehyde-3-phosphate dehydrogenase; GAS, gastrocnemius; HRT, heart; MDX, muscular dystrophy X linked; SD, standard deviation; TA, tibialis anterior; TRI, triceps.

time points, consistent with protein expression measured by western blot (Fig. 2C, D, and E). These data demonstrate sustained micro-dystrophin expression following delandistrogene moxeparvovec therapy in DMD^{MDX} rats.

Fibrosis quantification

Untreated DMD^{MDX} rats exhibited increased fibrosis in skeletal and cardiac muscle at 12 weeks versus WT rats, confirming that DMD-related remodeling occurs as early as 12 weeks (Fig. 3A). At all time points, delandistrogene moxeparvovec treatment led to a significant reduction in skeletal muscle (gastrocnemius) fibrosis in DMD^{MDX} rats (Fig. 3A and B), indicating a profound benefit in preventing dystrophic remodeling in skeletal muscle.

Cardiac tissue in saline-treated DMD^{MDX} rats trended toward increased fibrosis versus WT at all time points (WT 12 weeks vs. 12-, 24-, and 52-weeks saline-treated rats). Delandistrogene moxeparvovec treatment led to a trend toward reduced cardiac fibrosis in DMD^{MDX} rats at all time points evaluated. No adverse elevation in fibrosis levels or cardiac damage was observed in response to delandistrogene moxeparvovec treatment at all time points examined.

Histopathology

A reduction in skeletal muscle central nucleation (CN) was observed in delandistrogene moxeparvovec-treated DMD^{MDX} rats, indicative of reduced muscle degeneration versus saline-treated animals (Supplementary Fig. S3A and B). Overall, the 12-, 24-, and 52-week cohorts of saline-treated DMD^{MDX} rats exhibited a mean percent positive CN of >50%, whereas delandistrogene moxeparvovec-treated rats were <25% (Supplementary Fig. S3B). Furthermore, there were no signs of pathological effects related to delandistrogene moxeparvovec treatment in cardiac tissue.

Echocardiography

To avoid early mortality due to prolonged anesthesia exposure during echocardiography and facilitate a higher number of rats per experimental condition, echocardiography was limited to baseline and 52-week assessment.

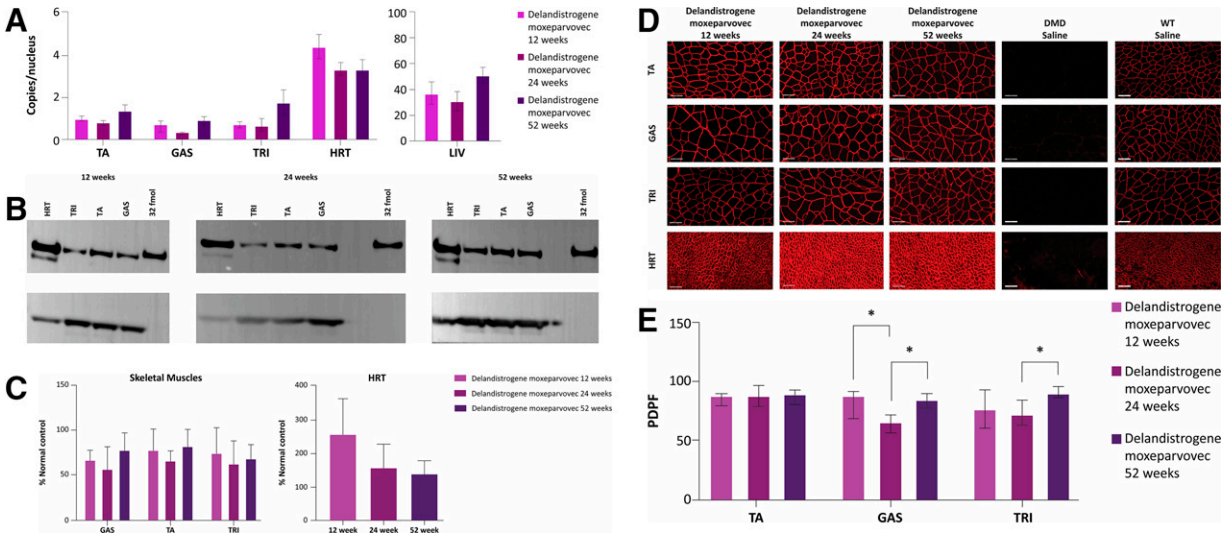

Figure 2. Delandistrogene moxeparvovec vector transduction and micro-dystrophin protein expression 12-, 24-, and 52-weeks following treatment in DMD^{MDX} rats. **(A)** Representative histogram illustrating vector biodistribution by ddPCR at 12, 24, and 52 weeks after delandistrogene moxeparvovec treatment in skeletal muscle, heart, and liver of DMD^{MDX} rats. Controls (saline-treated WT and DMD^{MDX} rats) had 0 copies/nucleus of vector DNA and therefore were not included for graphical representation. Bars represent mean ± SD. Statistical analysis: data were log-transformed (TA and TRI only) and analyzed using a one-way ANOVA. **(B)** Representative western blot images in delandistrogene moxeparvovec and cardiac muscle at 12, 24, and 52 weeks; corresponding protein bands illustrate expression of delandistrogene moxeparvovec micro-dystrophin. **(C)** Western blot quantification of delandistrogene moxeparvovec micro-dystrophin protein expression in muscle and heart represented as percent (%) of normal control at 12, 24, and 52 weeks. Bars represent mean ± SD. Statistical analysis: data were log-transformed heart only and analyzed using a one-way ANOVA. **(D)** Representative IF images for delandistrogene moxeparvovec and saline-treated DMD^{MDX} rats in various skeletal muscles and heart at 12-, 24-, and 52-weeks post dosing. Red labeling indicates delandistrogene moxeparvovec micro-dystrophin protein expression. **(E)** Quantification percent (%) delandistrogene moxeparvovec PDPF in skeletal muscles at 12, 24, and 52 weeks. Bars represent mean ± SD. Statistical analysis: data were analyzed using a one-way ANOVA (TA and TRI) or Kruskal–Wallis test (gastrocnemius) followed by a *post hoc* Tukey or Dunn's test, respectively (if applicable). Twelve-week delandistrogene moxeparvovec-treated cohort, $n = 10$; 24-week delandistrogene moxeparvovec-treated cohort, $n = 6$–8; 52-week delandistrogene moxeparvovec-treated cohort, $n = 3$–8. ANOVA, analysis of variance; ddPCR, droplet digital polymerase chain reaction; DMD, Duchenne muscular dystrophy; DYS3, dystrophin antibody 3; fmol, femtomole; GAPDH, glyceraldehyde-3-phosphate dehydrogenase; GAS, gastrocnemius; HRT, heart; IF, immunofluorescence; LIV, liver; MDX, muscular dystrophy X linked; PDPF, percentage micro-dystrophin-positive fibers; SD, standard deviation; TA, tibialis anterior; TRI, triceps; WT, wild type. $^*p < 0.05$.

Untreated DMD^{MDX} rats progressed toward cardiac dilation at 52 weeks, with a trend toward increased end-systolic volume (ESV) and significant reductions in left ventricular anterior wall (LVAW) and left ventricular posterior wall (LVPW) thickness (mm) systole compared with WT saline-treated rats (Fig. 4A, Supplementary Table S3). Delandistrogene moxeparvovec treatment attenuated dystrophic-related cardiac remodeling and restored LVAW systole and LVPW systole in DMD^{MDX} rats (Fig. 4A, Supplementary Table S3). No significant differences in ESV, LVAW, and LVPW were observed between WT and delandistrogene moxeparvovec-treated cohorts (Fig. 4A I–III). Furthermore, no differences were observed in isovolumic relaxation time (IVRT), end-diastolic volume, or LVPW and LVAW diastolic wall thickness between delandistrogene moxeparvovec-treated DMD^{MDX} and WT rats (Supplementary Fig. S4).

In alignment with structural aberrations and progression toward dystrophic cardiomyopathy, DMD^{MDX} rats had impaired cardiac function, demonstrated by significant reductions in ejection fraction and fractional shortening versus WT rats (Fig. 4A V–VI). Importantly, delandistrogene moxeparvovec led to a significant increase in ejection fraction and fractional shortening to WT levels in DMD^{MDX} rats 52 weeks post-treatment (Fig. 4A V–VI). Taken together, these results highlight the cardiac efficacy of delandistrogene moxeparvovec in attenuating cardiomyopathy in DMD^{MDX} rats.

Cardiomyocyte contractility and calcium handling

Cardiomyocytes from saline-control DMD^{MDX} rats had impaired contractile function, characterized by a significant decrease in sarcomere length amplitude and percent sarcomere shortening versus WT myocytes (Fig. 4B, I–III, Supplementary Table S4). Additionally, DMD^{MDX} cardiomyocyte contractile speed was impaired, as indicated by a trend toward an increase in time to peak 90% (TTP90) and a significant increase in sarcomere length time to return to baseline 90% (TTB90) (Fig. 4B, IV–V, Supplementary Table S4). Delandistrogene moxeparvovec significantly improved cardiomyocyte contractile response (to near WT levels) in DMD^{MDX} myocytes, as demonstrated by a significant increase in sarcomere length peak height, percent sarcomere shortening, and a reduction in

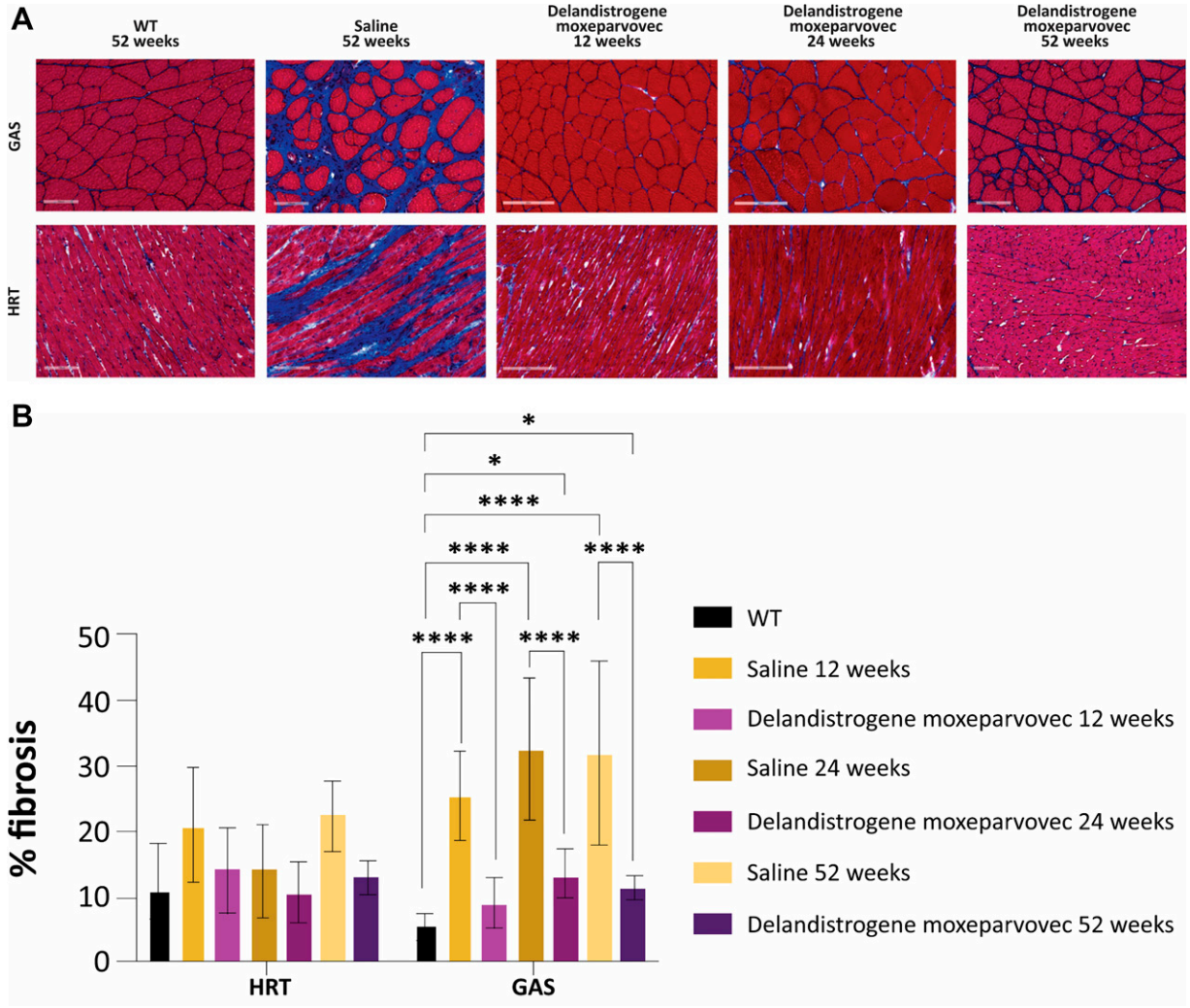

Figure 3. Fibrotic remodeling in skeletal muscle and heart of DMD^{MDX} rats and impact of delandistrogene moxeparvovec treatment. **(A)** Representative Masson's trichrome images illustrating fibrosis in gastrocnemius and heart after delandistrogene moxeparvovec or saline treatment, 12-, 24-, and 52-weeks post dosing in DMD^{MDX} rats. Blue staining indicates collagen deposition (fibrosis). **(B)** Quantification of percent (%) fibrosis in heart and gastrocnemius muscle. Bars represent mean ± SD. Statistical analysis: data were log-transformed and analyzed using a two-way ANOVA followed by a *post hoc* Tukey test. Statistics only shown for comparisons to WT or saline-treated DMD^{MDX} rats (within the same time point). Twelve-week delandistrogene moxeparvovec-treated cohort, $n = 10$; 12-week saline-treated cohort, $n = 6$–8; 24-week delandistrogene moxeparvovec-treated cohort, $n = 6$; 24-week saline-treated cohort, $n = 5$; 52-week delandistrogene moxeparvovec-treated cohort, $n = 3$–8; 52-week saline-treated cohort, $n = 4$–7; 52-week WT saline-treated cohort, $n = 2$–3. ANOVA, analysis of variance; DMD, Duchenne muscular dystrophy; GAS, gastrocnemius; HRT, heart; MDX, muscular dystrophy X linked; SD, standard deviation; WT, wild type. *$p < 0.05$, ****$p < 0.0001$.

sarcomere length TTB90 (Fig. 4B, II–V, Supplementary Table S4). However, sarcomere contractility (sarcomere length peak height and percent shortening) was significantly increased in WT versus delandistrogene moxeparvovec-treated cardiomyocytes (Fig. 4B, II–III).

DMD^{MDX} cardiomyocytes had impaired calcium handling, illustrated by a slower return to baseline 90% repolarization versus WT myocytes (Fig. 4B, VI–X, Supplementary Table S4). Significant decreases were observed in basal calcium levels in saline-treated DMD^{MDX} myocytes compared with WT. Myocytes treated with delandistrogene moxeparvovec normalized resting calcium levels to WT levels in DMD^{MDX} rats (Fig. 4B, VII). Delandistrogene moxeparvovec led to a significant increase in calcium transient peak height with a concomitant reduction in calcium transient time to baseline 90% versus DMD^{MDX} myocytes (Fig. 4B, VIII–X). In addition, delandistrogene moxeparvovec normalized calcium time to 90% depolarization (TTP90) to WT levels in DMD^{MDX} rat cardiomyocytes (Fig. 4B, IX–X).

Serum biomarkers

Serum cardiac troponin I (cTnI) was measured to evaluate cardiovascular pathology and response to delandistrogene moxeparvovec 12- and 52-weeks post-treatment (Supplementary Fig. S5A). At week 12, a significant elevation in cTnI levels was observed in saline-treated DMD^{MDX} rats. Delandistrogene moxeparvovec treatment

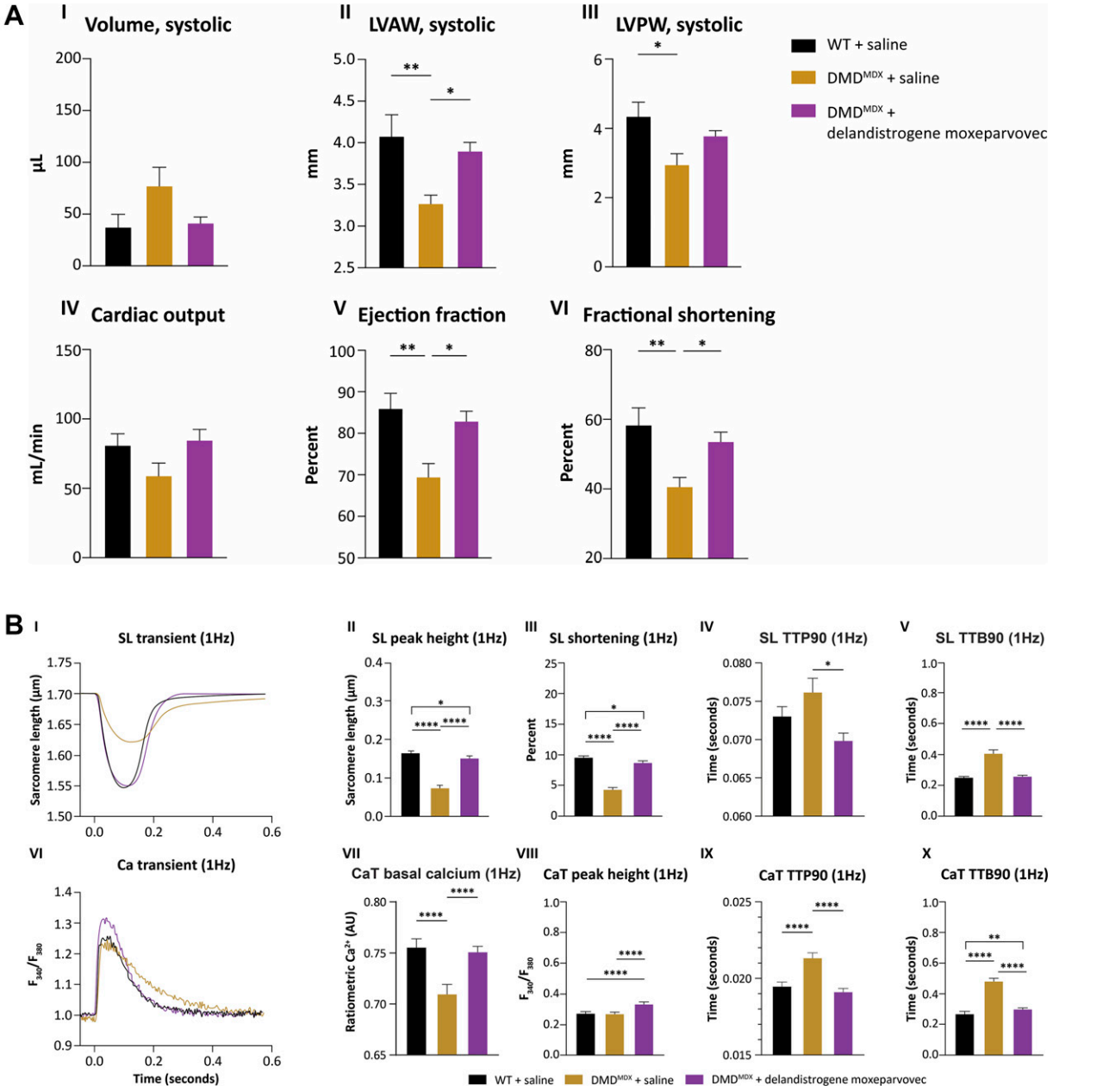

Figure 4. Cardiac echocardiography and cardiomyocyte functional measurements in DMD^{MDX} rats treated with delandistrogene moxeparvovec. **(A)** Echocardiography measurements in DMD^{MDX} rats 52 weeks following delandistrogene moxeparvovec treatment: (I) end-systolic volume; (II) LVAW, systole; (III) LVPW, systole; (IV) cardiac output; (V) ejection fraction; (VI) fractional shortening. Bars represent mean ± SEM. Statistical analysis: data were log-transformed (systolic volume only) and analyzed using a one-way ANOVA followed by a *post hoc* Tukey test (if applicable). **(B)** Cardiomyocyte contractile function and Ca^{2+} handling after delandistrogene moxeparvovec treatment in DMD^{MDX} rats: (I) representative sarcomere length transients from experimental cohorts at 52 weeks; (II) sarcomere length peak height; (III) sarcomere length percent (%) shortening; (IV) sarcomere length time to reach 90% peak depolarization; (V) sarcomere length time to return to baseline 90% repolarization; (VI) representative calcium transient traces from experimental cohorts at 52 weeks; (VII) basal calcium; (VIII) calcium transient peak height; (IX) calcium transient time to reach 90% peak depolarization; (X) calcium transient time to return to baseline 90% repolarization. Bars represent mean ± SEM. Statistical analysis: data were analyzed using Kruskal–Wallis test followed by a *post hoc* Dunn's test. Twelve-week delandistrogene moxeparvovec-treated cohort, $n = 10$; 52-week delandistrogene moxeparvovec-treated cohort, $n = 6$ (299–337 cardiomyocytes); 52-week saline-treated cohort, $n = 7$ (112–136 cardiomyocytes); 52-week WT saline-treated cohort, $n = 5$ (255–275 cardiomyocytes). ANOVA, analysis of variance; Ca^{2+}, calcium; CaT, Ca^{2+} transient; DMD, Duchenne muscular dystrophy; F_{340}/F_{380}, ratiometric peak height of Ca^{2+} transient; LVAW, left ventricular anterior wall; LVPW, left ventricular posterior wall; MDX, muscular dystrophy X linked; SEM, standard error of the mean; SL, sarcomere length; TTB90, time to baseline 90%; TTP90, time to peak 90%; WT, wild type. $^{*}p < 0.05$; $^{**}p < 0.01$; $^{****}p < 0.0001$.

led to a significant reduction in cTnI in DMD^{MDX} rats 12 weeks post-treatment (Supplementary Fig. S5A). At 52 weeks, delandistrogene moxeparvovec treatment showed a reduction in cTnI levels; however, the reduction was not statistically significant versus that in saline-treated DMD^{MDX} rats (Supplementary Fig. S5A).

Elevated levels of creatine kinase (CK), aspartate aminotransferase, and alanine aminotransferase reflect muscle damage and are considered biomarkers of the muscular pathology in DMD.[2] Evaluation of these clinical biochemical parameters revealed reductions in CK at week 12, aspartate aminotransferase at weeks 12 and 52, and alanine aminotransferase at week 12 in delandistrogene moxeparvovec-treated DMD^{MDX} rats versus saline-treated rats (Supplementary Fig. S5B–D). Due to varying levels of hemolysis across treatment groups, CK measurements at weeks 24 and 52 were not assessed.

Activity cage assessments

A statistically significant increase in horizontal ambulation and vertical activity was demonstrated at 12 weeks post-treatment in delandistrogene moxeparvovec-treated DMD^{MDX} rats versus saline controls (Supplementary Fig. S6). Delandistrogene moxeparvovec treatment led to a trend toward improved ambulation at 52 weeks (Supplementary Fig. S6). These data demonstrate functional improvement in mobility in DMD^{MDX} rats after delandistrogene moxeparvovec treatment. The noted decline in ambulatory performance across all experimental groups from 12 and 52 weeks could be due to the size constraints of the activity cage, sensitivity of the assay, and age of the animal.

Transduction of AAVrh74.MHCK7.GFP in cardiomyocyte cells

To further understand the effect of delandistrogene moxeparvovec treatment on cardiac function in human cells, transduction of a reporter construct AAVrh74.MHCK7.GFP was evaluated in human induced pluripotent stem cell cardiomyocytes (hiPSC). Expression of green fluorescent protein in hiPSC cardiomyocytes treated with AAVrh74.MHCK7.GFP indicated that the Myosin Heavy Chain Creatine Kinase promoter (MHCK7) promoter effectively transduced and expressed the GFP transgene in human cardiomyocytes. In congruence with MHCK7 derived *in vivo* data, an *in vitro* reporter-based assay with AAVrh74.MHCK7.eGFP led to increased GFP expression in hiPSC cardiomyocytes. These data confirm that MHCK7 can express a transgene payload in human cardiomyocytes (Supplementary Fig. S7A and B).

DISCUSSION

Cardiomyopathy has become the most common cause of death in patients with DMD.[6,7] This study was designed to evaluate the cardiovascular efficacy of delandistrogene moxeparvovec in a more suitable model of cardiomyopathy, the DMD^{MDX} rat. Delandistrogene moxeparvovec contains the MHCK7 promoter, which includes an alpha-myosin heavy chain enhancer to drive a high level of expression in the heart.[16,24] This purposeful design was intended to provide protection against cardiomyopathy. This study provides the first direct evidence for the biological activity of delandistrogene moxeparvovec micro-dystrophin in the heart with a demonstration of robust expression and significant improvements in cardiac measures.

Importantly, treatment with delandistrogene moxeparvovec extended the life expectancy of DMD^{MDX} rats, prolonging survival to that of WT Sprague-Dawley rats.[25] In addition, improved ambulation was observed in treated rats versus saline controls, which illustrates the skeletal muscle efficacy of delandistrogene moxeparvovec and supports the improved functional data seen in clinical trials.

Treatment with delandistrogene moxeparvovec demonstrated improvements in muscle integrity, with reductions in fibrosis seen at all time points across skeletal and cardiac muscle. Additionally, similar findings have been reported in a recent study, highlighting fibrosis as a consistent pathological hallmark of DMD.[26] The reduction in fibrosis suggests that delandistrogene moxeparvovec attenuates the dystrophic remodeling characteristic of DMD. Additionally, decreased CN with delandistrogene moxeparvovec treatment reflects improvement in muscle regeneration and reduction in muscle degeneration.

This study allowed for a comprehensive analysis of delandistrogene moxeparvovec micro-dystrophin protein expression and localization across all tissues including the heart. Delandistrogene moxeparvovec vector biodistribution and micro-dystrophin expression evaluated by droplet digital polymerase chain reaction and western blot, indicated biodistribution and robust expression across tissues and time points. Our findings are in line with a similar AAV-based gene therapy assessed in the same DMD^{MDX} rat model.[26] Biodistribution, protein expression, and histological parameters were consistent across the 12-, 24-, and 52-week time points, indicating long-term durability of delandistrogene moxeparvovec treatment. The durability of cardiac micro-dystrophin expression at week 52 supports the efficacy of delandistrogene moxeparvovec in improving cardiac function and reversing adverse cardiac remodeling in DMD^{MDX} rats.

Since cardiomyopathy is a significant contributor to morbidity and mortality in patients with DMD,[27] the efficacy of delandistrogene moxeparvovec in the heart was evaluated. A key characteristic of heart failure is abnormal calcium transients, which often have diminished amplitude and are prolonged in ventricular cardiomyocytes of patients.[18] These changes at the cardiomyocyte level are causative for impaired cardiac function.[18] Here we show that delandistrogene moxeparvovec treatment enhances cardiomyocyte contractility and normalizes calcium handling in DMD^{MDX} rats as a result of membrane stabilization *via* delandistrogene moxeparvovec micro-dystrophin cardiac expression. The precise mechanism regarding calcium stabilization following delandistrogene moxeparvovec treatment is not completely understood. Based on our data from isolated ventricular cardiomyocytes, the delandistrogene

moxeparvovec micro-dystrophin construct enhances the amplitude of calcium transients and reduces the transient return to baseline speed. The construct contains key regions of the full dystrophin protein (ABD-H1-R1-R3-H2-R24-H4-CR) that have been shown to reduce basal calcium levels in DMD^{MDX} rats.[28] These data indicate that upstream micro-dystrophin construct elements are sufficient to improve calcium handling in DMD^{MDX} rats.

Previous studies have characterized diastolic and systolic dysfunction in DMD^{MDX} rats as early as 12 weeks, depending on time point and treatment, highlighting the progressive nature of cardiac impairment in this model.[17,18,26,28] Data from our echocardiography analysis revealed improved indicators of cardiac systolic function with delandistrogene moxeparvovec 52 weeks post-treatment versus saline controls. For diastolic dysfunction, data at 52 weeks indicated an improvement in isovolumetric relaxation time in DMD^{MDX} rats treated with delandistrogene moxeparvovec.

This study demonstrated that delandistrogene moxeparvovec micro-dystrophin was well tolerated in rats with no evidence of toxicity. Our findings show that long-term treatment of DMD^{MDX} rats with delandistrogene moxeparvovec micro-dystrophin at a clinical dose level (1.33×10^{14} vg/kg) did not lead to adverse cardiac events or dilated cardiomyopathy progression. Cardiac toxicity following gene therapy may be transgene expression dependent,[2,29] and the threshold of expression required to reach toxicity in the human heart versus a rodent model may differ.[30] Hart et al. (2022) observed cardiac toxicity in a DMD mouse model (D2.*mdx* mouse) due to a 55-fold increase in micro-dystrophin expression in the heart.[29] In contrast, our study achieved one-to-two-fold higher cardiac expression in DMD^{MDX} rats compared with WT, resulting in functional improvements at the cardiomyocyte and whole-heart levels. Importantly, our findings indicate enhanced survival rates, with no reported cardiac events or fatalities in DMD^{MDX} rats treated with delandistrogene moxeparvovec.

Limitations

There are certain limitations of this study that should be considered. The specific causes of death of study animals were not evaluated. However, the improvement in survival observed in delandistrogene moxeparvovec-treated DMD^{MDX} rats is a clear demonstration of a treatment-related effect.

Functional analysis at intermediate time points (24, 36, and 48 weeks) could have offered a more expansive view of the trajectory of motor function decline within the DMD^{MDX} rats. In addition, reduced animal viability over 52 weeks, particularly in untreated rats, limited the study to small cohorts (approximately six to eight animals). Consequently, the variability in echocardiography and the small sample size may have contributed to the reduced significance observed in several measures.

CONCLUSIONS

This study provides evidence for the biological activity of delandistrogene moxeparvovec micro-dystrophin in the heart and skeletal muscles of DMD^{MDX} rats. These data demonstrate a previously undescribed role for this therapy in improving cardiac function and support delandistrogene moxeparvovec treatment for DMD.

AUTHORS' CONTRIBUTIONS

Conceptualization: R.A.P. Methodology: S.B., C.W., L.L., G.C.-O., A.K., A.H., J.E., A.F., E.N., R.A.P. Formal analysis: S.B., C.W., L.L., G.C.-O., A.K., A.H., J.E. Investigation: S.B., C.W., L.L., G.C.-O., A.K., A.H., J.E., A.F. Resources: L.R.R.-K., R.A.P. Writing—original draft: S.B., C.W., G.C.-O., R.A.P. Writing—review and editing: S.B., C.W., L.L., G.C.-O., A.K., A.H., J.E., A.F., E.N., L.R.R.-K., R.A.P. Visualization: S.B, C.W., G.C.-O., R.A.P. Supervision: L.R.R.-K., R.A.P. Project administration: E.N., R.A.P.

AUTHOR DISCLOSURE

S.B., C.W., L.L., G.C.-O., A.K., A.H., J.E., A.F., E.N., L.R.R.-K., and R.A.P. are employees of Sarepta Therapeutics and may have stock options. L.R.R.-K. is a co-inventor of AAVrh74.MHCK7.micro-dys technology.

FUNDING INFORMATION

This research is funded by Sarepta Therapeutics. Writing and editorial assistance were provided by Ayesha Babar, MSc, of Nucleus Global, in accordance with Good Publication Practice (GPP) 2022 guidelines (https://www.ismpp.org/gpp-2022), and were funded by Sarepta Therapeutics Inc., Cambridge, MA, USA.

SUPPLEMENTARY MATERIAL

Supplementary Figure S1
Supplementary Figure S2
Supplementary Figure S3
Supplementary Figure S4
Supplementary Figure S5
Supplementary Figure S6
Supplementary Figure S7
Supplementary Table S1
Supplementary Table S2
Supplementary Table S3
Supplementary Table S4
Supplementary Appendix SA1

REFERENCES

1. Elangkovan N, Dickson G. Gene therapy for Duchenne muscular dystrophy. J Neuromuscul Dis 2021;8(s2):S303–S316; doi: 10.3233/JND-210678
2. Duan D, Goemans N, Takeda S, et al. Duchenne muscular dystrophy. Nat Rev Dis Primers 2021; 7(1):13; doi: 10.1038/s41572-021-00248-3
3. McNally EM. Cardiomyopathy in muscular dystrophy: When to treat? JAMA Cardiol 2017;2(2): 199; doi: 10.1001/jamacardio.2016.4910
4. Broomfield J, Hill M, Guglieri M, et al. Life expectancy in Duchenne muscular dystrophy: Reproduced individual patient data meta-analysis. Neurology 2021;97(23):e2304–e2314; doi: 10.1212/wnl.0000000000012910
5. Ryder S, Leadley RM, Armstrong N, et al. The burden, epidemiology, costs and treatment for Duchenne muscular dystrophy: An evidence review. Orphanet J Rare Dis 2017;12(1):79; doi: 10.1186/s13023-017-0631-3
6. Schultz TI, Raucci FJ, Jr, Salloum FN. Cardiovascular disease in Duchenne muscular dystrophy: Overview and insight into novel therapeutic targets. JACC Basic Transl Sci 2022;7(6): 608–625; doi: 10.1016/j.jacbts.2021.11.004
7. Zhang H, Zhan Q, Huang B, et al. AAV-mediated gene therapy: Advancing cardiovascular disease treatment. Front Cardiovasc Med 2022;9: 952755; doi: 10.3389/fcvm.2022.952755
8. Law ML, Cohen H, Martin AA, et al. Dysregulation of calcium handling in Duchenne muscular dystrophy-associated dilated cardiomyopathy: Mechanisms and experimental therapeutic strategies. J Clin Med 2020;9(2); doi: 10.3390/jcm9020520
9. US Food & Drug Administration. ELEVIDYS Highlights of Prescribing Information 2023. Available from: https://www.fda.gov/media/169679/download [Last accessed: September, 2023].
10. Sarepta Therapeutics. Sarepta Therapeutics Announces FDA Approval of ELEVIDYS, the First Gene Therapy to Treat Duchenne Muscular Dystrophy 2023. Available from: https://investorrelations.sarepta.com/news-releases/news-release-details/sarepta-therapeutics-announces-fda-approval-elevidys-first-gene [Last accessed: July, 2023].
11. UAE Ministry of Health & Prevention. Registered Medical Product Directory Dubai. UAE Ministry of Health and Prevention; 2023. Available from: https://mohap.gov.ae/en/services/registered-medical-product-directory [Last accessed: February, 2024].
12. NHRA Bahrain. Pharmacy & Pharmaceutical Products Regulation (PPR) 2024. Available from: https://www.nhra.bh/Departments/PPR/ [Last accessed: February, 2024].
13. Kuwait Ministry of Health. Drug and Dietary Supplement Price List. 2024. Available from: https://e.gov.kw/sites/kgoenglish/Pages/eServices/MOH/DrugFoodSupplementPrices.aspx (Last accessed: February, 2024).
14. Qatar Ministry of Public Health. Qatar National Formulary. 2024. Available from: https://www.moph.gov.qa/english/OurServices/advancedsearch/Pages/servicesdetails.aspx?serviceId=234 (Last accessed: February, 2024).
15. Mendell J, Sahenk Z, Lehman K, et al. Assessment of systemic delivery of rAAVrh74.MHCK7.micro-dystrophin in children with Duchenne muscular dystrophy: A nonrandomized controlled trial. JAMA Neurol 2020;77(9):1122–1131; doi: 10.1001/jamaneurol.2020.1484
16. Potter RA, Griffin DA, Heller KN, et al. Dose-escalation study of systemically delivered rAAVrh74.MHCK7.micro-dystrophin in the mdx mouse model of Duchenne muscular dystrophy. Hum Gene Ther 2021;32(7–8):375–389; doi: 10.1089/hum.2019.255
17. Larcher T, Lafoux A, Tesson L, et al. Characterization of dystrophin deficient rats: A new model for Duchenne muscular dystrophy. PLoS One 2014;9(10):e110371; doi: 10.1371/journal.pone.0110371
18. Szabó PL, Ebner J, Koenig X, et al. Cardiovascular phenotype of the Dmd(mdx) rat - a suitable animal model for Duchenne muscular dystrophy. Dis Model Mech 2021;14(2):dmm047704; doi: 10.1242/dmm.047704
19. Yucel N, Chang AC, Day JW, et al. Humanizing the mdx mouse model of DMD: The long and the short of it. NPJ Regen Med 2018;3:4; doi: 10.1038/s41536-018-0045-4
20. Bulfield G, Siller WG, Wight PA, et al. X chromosome-linked muscular dystrophy (mdx) in the mouse. Proc Natl Acad Sci U S A 1984; 81(4):1189–1192; doi: 10.1073/pnas.81.4.1189
21. Nakamura K, Fujii W, Tsuboi M, et al. Generation of muscular dystrophy model rats with a CRISPR/Cas system. Sci Rep 2014;4:5635; doi: 10.1038/srep05635
22. Baine S, Bonilla I, Belevych A, et al. Pyridostigmine improves cardiac function and rhythmicity through RyR2 stabilization and inhibition of STIM1-mediated calcium entry in heart failure. J Cell Mol Med 2021;25(10):4637–4648; doi: 10.1111/jcmm.16356
23. Wright PT, Tsui SF, Francis AJ, et al. Approaches to high-throughput analysis of cardiomyocyte contractility. Front Physiol 2020;11: 612; doi: 10.3389/fphys.2020.00612
24. Salva MZ, Himeda CL, Tai PW, et al. Design of tissue-specific regulatory cassettes for high-level rAAV-mediated expression in skeletal and cardiac muscle. Mol Ther 2007;15(2):320–329; doi: 10.1038/sj.mt.6300027
25. Altun M, Bergman E, Edström E, et al. Behavioral impairments of the aging rat. Physiol Behav 2007;92(5):911–923; doi: 10.1016/j.physbeh.2007.06.017
26. Le Guiner C, Xiao X, Larcher T, et al. Evaluation of an AAV9-mini-dystrophin gene therapy candidate in a rat model of Duchenne muscular dystrophy. Mol Ther Methods Clin Dev 2023;30: 30–47; doi: 10.1016/j.omtm.2023.05.017
27. Yamamoto T, Awano H, Zhang Z, et al. Cardiac dysfunction in Duchenne muscular dystrophy is less frequent in patients with mutations in the dystrophin Dp116 coding region than in other regions. Circ Genom Precis Med 2018;11(1):e001782; doi: 10.1161/circgen.117.001782
28. Bourdon A, François V, Zhang L, et al. Evaluation of the dystrophin carboxy-terminal domain for micro-dystrophin gene therapy in cardiac and skeletal muscles in the DMD(mdx) rat model. Gene Ther 2022;29(9):520–535; doi: 10.1038/s41434-022-00317-6
29. Hart CC, Lee IL, Xie J, et al. Potential limitations of micro-dystrophin gene therapy for Duchenne muscular dystrophy. bioRxiv 2022; doi: 10.1101/2022.10.02.510519
30. Nair AB, Jacob S. A simple practice guide for dose conversion between animals and human. J Basic Clin Pharm 2016;7(2):27–31; doi: 10.4103/0976-0105.177703
31. Rodino-Klapac LR, Janssen PML, Montgomery CL, et al. A translational approach for limb vascular delivery of the micro-dystrophin gene without high volume or high pressure for treatment of Duchenne muscular dystrophy. J Transl Med 2007;5:45; doi: 10.1186/1479-5876-5-45
32. Sondergaard PC, Griffin DA, Pozsgai ER, et al. AAV.Dysferlin overlap vectors restore function in Dysferlinopathy animal models. Ann Clin Transl Neurol 2015;2(3):256–270; doi: 10.1002/acn3.172
33. Schnepp BC, Jensen RL, Chen CL, et al. Characterization of adeno-associated virus genomes isolated from human tissues. J Virol 2005; 79(23):14793–14803; doi: 10.1128/JVI.79.23.14793-14803.2005
34. Mendell JR, Rodino-Klapac LR, Rosales XQ, et al. Sustained alpha-sarcoglycan gene expression after gene transfer in limb-girdle muscular dystrophy, type 2D. Ann Neurol 2010;68(5): 629–638; doi: 10.1002/ana.22251
35. Rafael JA, Sunada Y, Cole NM, et al. Prevention of dystrophic pathology in mdx mice by a truncated dystrophin isoform. Hum Mol Genet 1994;3(10):1725–1733; doi: 10.1093/hmg/3.10.1725
36. Phelps SF, Hauser MA, Cole NM, et al. Expression of full-length and truncated dystrophin mini-genes in transgenic mdx mice. Hum Mol Genet 1995;4(8):1251–1258; doi: 10.1093/hmg/4.8.1251

37. Gregorevic P, Allen JM, Minami E, et al. rAAV6-microdystrophin preserves muscle function and extends lifespan in severely dystrophic mice. Nat Med 2006;12(7):787–789; doi: 10.1038/nm1439

38. Mendell JR, Shieh PB, McDonald CM, et al. Expression of SRP-9001 dystrophin and stabilization of motor function up to 2 years post-treatment with delandistrogene moxeparvovec gene therapy in individuals with Duchenne muscular dystrophy. Front Cell Dev Biol 2023; 11:1167762; doi: 10.3389/fcell.2023.1167762

39. Asher DR, Thapa K, Dharia SD, et al. Clinical development on the frontier: Gene therapy for Duchenne muscular dystrophy. Expert Opin Biol Ther 2020;20(3):263–274; doi: 10.1080/14712598.2020.1725469

40. Zheng C, Baum BJ. Evaluation of promoters for use in tissue-specific gene delivery. Methods Mol Biol 2008;434:205–219; doi: 10.1007/978-1-60327-248-3_13

41. Chandler RJ, Venditti CP. Gene therapy for metabolic diseases. Transl Sci Rare Dis 2016;1(1): 73–89; doi: 10.3233/trd-160007

Received for publication January 30, 2024;
accepted after revision October 15, 2024.

Published online: November 28, 2024.